Synthesis, Characterization, and Catalytic Activities for the Polymerization of Olefins Promoted by Zirconium(III) and Titanium(III) Allyl Complexes

Biswajit Ray, Tali Gueta Neyroud, Moshe Kapon, Yoav Eichen, and Moris S. Eisen*

Department of Chemistry and Institute of Catalysis Science and Technology, Technion—Israel Institute of Technology, Technion City, Haifa 32000, Israel

Received November 21, 2000

The reaction of early-transition-metal halides MCl_4 (M = Zr, Ti) with 2 equiv of the lithium allyl compound $(^tBuMe_2SiCH)_2CHLi\cdot TMEDA$ in toluene produced the corresponding reduced complexes $[\{(^tBuMe_2SiCH)_2CH\}_2M(\mu\text{-}Cl)_2Li\cdot TMEDA]$ (M = Zr (**1**), Ti (**2**)), that were isolated as air-sensitive dark brown (Zr) and brick red (Ti) crystals in 48% and 42% yield, respectively. In addition, each reaction is associated with the formation of the dimer of the allyl ligand (**3**). Complexes **1** and **2** and dimer **3** were fully characterized spectroscopically, including solid-state X-ray diffraction studies. Complex **1** represents the first solid-state characterization for a Zr(III)−allyl complex. Oxidation of complexes **1** and **2** allows the formation of the corresponding neutral complexes $\{(^tBuMe_2SiCH)_2CH\}_2MCl_2$ (M = Zr (**4**), Ti **5**)), which were isolated as air-sensitive light yellow (Zr) and orange (Ti) powders in 23% and 11% yields, respectively. The allylic moieties in complex **5** showed a dynamic interconverting coordination from η^3 to η^1, causing an alternation between C_2 and C_{2v} symmetries of the complex. For the cationic complex **4** a similar dynamic interconverting coordination from η^3 to η^1 was observed. The catalytic activities of complexes **1** and **2** activated with MAO in the polymerization of propylene and ethylene were studied. The activity of complexes **1** and **2** was compared to the corresponding activities presented by complexes **4** and **5**, respectively, indicating that during the polymerization process, Zr(III) and Ti(III) are oxidized to the corresponding cationic Zr(IV) and Ti(IV) species. For propylene, an elastomeric polypropylene was obtained, whereas for ethylene high-density polyethylene was produced. When the η^3 coordination modes of the ligands are operative in the complex, a cationic racemic octahedral compound is formed, which is responsible for the polymerization of the isotactic domains, whereas when the η^1 coordination modes of the ligands are effective, a cationic tetrahedral complex is obtained, accounting for the atactic domains. The formations of isotactic−atactic domains within a polymer chain give rise to elastomeric polypropylene.

Introduction

Great advancement has been made in the design and synthesis of "well defined" single and geometry-constrained catalysts for the polymerization of olefins.[1−5] Most of the catalysts belong either to the cyclopentadienyl (Cp)-based catalysts or to a combination of a Cp and a pendant amido ligand.[6−8] In the past decade, it has become evident that group 4 complexes without the cyclopentadienyl ancillary ligations have shown unique reactivities toward the polymerization of α-olefins. Diamido,[9−12] benzamidine,[13−19] dialkoxo,[20−23] borataben-

(1) (a) Bochmann, M. *J. Chem. Soc., Dalton Trans.* **1996**, 255. (b) Resconi, L.; Cavallo, L.; Fait, A.; Piemontesi, F. *Chem. Rev.* **2000**, *100*, 1253. (c) Coates, G. W. *Chem. Rev.* **2000**, *100*, 1223. (d) Alt, H. G.; Koppl, A. *Chem. Rev.* **2000**, *100*, 1205. (e) Boffa, L. S.; Novak, B. M. *Chem. Rev.* **2000**, *100*, 1479.

(2) (a) Brintzinger, H. H.; Fischer, D.; Mülhaupt, R.; Rieger, B.; Waymouth, R. M. *Angew. Chem., Int. Ed. Engl.* **1995**, *34*, 1143. (b) McKnight, A. L.; Waymouth, R. M. *Chem. Rev.* **1998**, *98*, 2587.

(3) Kaminsky, W. *Catal. Today* **1994**, *20*, 257.

(4) Möhring, R. C.; Conville, N. J. *J. Organomet. Chem.* **1994**, *479*, 1.

(5) (a) Marks, T. J. *Acc. Chem. Res.* **1992**, *25*, 57. (b) Chen, E. Y.-X.; Marks, T. J. *Chem. Rev.* **2000**, *100*, 1391.

(6) Mu, Y.; Piers, W. E.; McGillivray, L. R.; Zaworotko, M. J. *Polyhedron* **1995**, *14*, 1.

(7) Okuda, J. *Chem. Ber.* **1990**, *123*, 1649.

(8) Devore, D. D.; Timmers, F. J.; Hasha, D. L.; Rosen, R. K.; Marks, T. J.; Deck, P. A.; Stem, C. L. *Organometallics* **1995**, *14*, 3132 and references therein.

(9) Baumann, R.; Davis, W. M.; Schrock, R. R. *J. Am. Chem. Soc.* **1997**, *119*, 3830.

(10) Warren, T. H.; Schrock, R. R.; Davis, W. M. *Organometallics* **1996**, *15*, 562.

(11) Scollard, J. D.; McConville, D. H. *J. Am. Chem. Soc.* **1996**, *118*, 10008.

(12) Mack, H.; Eisen, M. S. *J. Organomet. Chem.* **1996**, *525*, 81.

(13) Averbuj, C.; Tish, E.; Eisen, M. S. *J. Am. Chem. Soc.* **1998**, *120*, 8640.

(14) Volkis, V.; Shmulinson, M.; Averbuj, C.; Lisovskii, A.; Edelmann, F. T.; Eisen, M. S. *Organometallics* **1998**, *17*, 3155.

(15) Herskovics-Korine, D.; Eisen, M. S. *J. Organomet. Chem.* **1995**, *503*, 307.

(16) Gomez, R.; Duchateau, R.; Chernega, A. N.; Meetsma, A.; Edelmann, F. T.; Teuben, J. H.; Green, M. L. H. *J. Chem. Soc., Dalton Trans.* **1995**, 217.

(17) Hagadorn, J. R.; Arnold, J. *Organometallics* **1994**, *13*, 4670.

(18) Walther, D.; Fischer, R.; Friedrich, M.; Gebhardt, P.; Görls, H. *Chem. Ber.* **1996**, *129*, 1389.

(19) Florez, J. C.; Chien, J. C. W.; Rausch, M. D. *Organometallics* **1995**, *14*, 2106.

10.1021/om0009942 CCC: $20.00
Publication on Web 06/15/2001

zene,[24,25] acetylacetonate,[26] and phosphinoamines[27] comprise some of the ancillary ligands that have been utilized in the synthesis of these group 4 complexes, alternatives to the metallocene catalysts.

Little attention has been paid to simple allylic ligands as spectators in the olefin polymerization process, due to their intrinsic higher reactivity and low thermal stability as compared to the Cp ligand.[28] Bochmann and co-workers[29] have recently reported moderate ethylene polymerization activity using zwitterionic diallylzirconium (IV) complexes (**A**) formed by the reaction of [Cp-

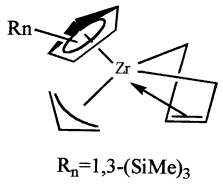

A

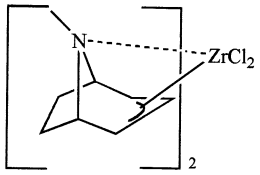

B

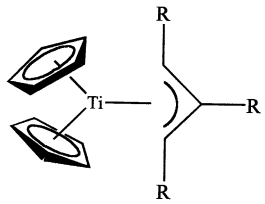

C

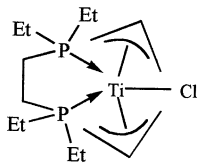

D

(allyl)Zr(dienyl)] and $B(C_6F_5)_3$ in toluene at −78 °C. The high polydispersity of the obtained polyethylenes suggested the loss of active site uniformity. Erker and coworkers have reported the synthesis and X-ray crystal structure for CpZr(η^3-allyl)(butadiene)[30] and CpZr(allyl)$_3$,[31] the latter exhibiting three different types of allylic ligations: σ-allyl, η^1-allyl, and η^3-allyl. Although the catalytic activity of these two complexes for the polymerization of α-olefins has not yet been reported. Bergman and Lavoie[32,33] have recently reported a Zr-(IV) complex containing a tropidinyl ligand as an alternative to cyclopentadienyl ligation, in which there is a nitrogen donating a free pair of electrons in addition to an allylic moiety, [(trop)$_2$ZrX$_2$] (**B**) (trop = tropidinyl and X = Cl). This complex, when activated by MAO, exhibits moderate ethylene polymerization activity (17 kg mol^{-1} h^{-1}). Interestingly, the mixed cyclopentadienyl tropidinyl zirconium dichloride shows very high activity for the polymerization of ethylene when activated with MMAO (9860 kg of polymer mol^{-1} h^{-1}).[34]

In general, early-transition-metal allyl complexes have an enormous practical importance as either catalyst precursors or stoichiometric reagents in the synthesis of organic compounds.[35−40] For example, allyltitanium complexes are important intermediates in the Ziegler−Natta polymerization of conjugated dienes,[41,42] in the isomerization of olefins,[43,44] and in the stereoselective synthesis of homoallyl alcohols[45] and their analogues.[46] For early-transition-metal group 4 complexes containing the allyl moiety, in the majority of these compounds the metals exhibit the higher oxidation state: e.g., +4. Very few well-characterized group 4 early-transition-metal allyl complexes in the +3 oxidation state are available in the literature, presumably due to their paramagnetic nature (reactivity) and the difficulty in handling these compounds. For Ti(III) allyl complexes, only three compounds have been characterized in the solid state. The first characterized compound was a mixed allyl cyclopentadienyl complex with the general structure Cp$_2$Ti(η^3-CHR$_1$CR$_2$CHR$_3$) (**C**).[47] Very recently two new titanium allyl complexes were also characterized in the solid state: the dinuclear mixed-valent Ti_2^{5+} species $Ti_2(\mu\text{-}Cl)_2Cl_2(dmpe)_2(\mu_2,\mu_3\text{-}C_2H_5)$ and the mononuclear $TiCl(Et_2PC_2H_4PEt_2)(\eta^3\text{-}C_3H_5)_2$ (**D**), which was stabilized by a neutral bis-phosphine (dmpe) ligand.[48]

Although some Ti(III)−allyl complexes have been fully characterized spectroscopically,[47,49−50] well-character-

(20) Linden, A. V. D.; Schaverien, C. J.; Meijboom, N.; Ganter, C.; Orpen, A. G. *J. Am. Chem. Soc.* **1995**, *117*, 3008.
(21) Fokken, S.; Spaniol, T. P.; Kang, H.-C.; Massa, W.; Okuda, J. *Organometallics* **1996**, *15*, 5069.
(22) Mack, H.; Eisen, M. S. *J. Chem. Soc., Dalton Trans.* **1998**, 917.
(23) Schrock, R. R.; Baumann, R.; Reid, S. M.; Goodman, J. T.; Stumpf, R.; Davis, W. M. *Organometallics* **1999**, *18*, 3649.
(24) Pellecchia, C.; Proto, A.; Longo, P.; Zambelli, A. *Macromol. Chem. Rapid Commun.* **1991**, *12*, 663.
(25) Pellecchia, C.; Proto, A.; Longo, P.; Zambelli, A. *Macromol. Chem. Rapid Commun.* **1992**, *13*, 277.
(26) Shmulinson, M.; Galan-Fereres, M.; Lisovskii, A.; Nelkenbaum, E.; Semiat, R.; Eisen, M. S. *Organometallics* **2000**, *19*, 1208.
(27) (a) Koch, T.; Blaurock, S.; Hey-Hawkins, E.; Galan-Fereres, M.; Plat, D.; Eisen, M. S. *J. Organomet. Chem.* **2000**, *595*, 126. (b) For metallocene-based elastomeric polypropylene, see: Coates, G. W.; Waymouth, R. M. *Science* **1995**, *267*, 217. (c) Hu, Y.; Krejchi, M. T.; Shah, C. D.; Myers, C. I.; Waymouth, R. M. *Macromolecules* **1998**, *31*, 6908 and references therein. (d) Carlson, E. D.; Krejchi, M. T.; Shah, C. D.; Terakawa, T.; Waymouth, R. M. *Macromolecules* **1998**, *31*, 5343 and references therein. (e) Bruce, M. D.; Waymouth, R. M. *Macromolecules* **1998**, *31*, 2707 and references therein. Kravchenko, R.; Masood, A.; Waymouth, R. M.; Myers, C. I. *J. Am. Chem. Soc.* **1998**, *120*, 2039.
(28) Pritovsck, G. J. P.; Gibson, V. C.; Wass, D. F. *Angew. Chem., Int. Ed.* **1999**, *38*, 428.
(29) Pindado, G. J.; Thornton-Pett, M.; Bouwkamp, M.; Meetsma, A.; Hessen, B.; Bochmann, M. *Angew. Chem., Int. Ed. Engl.* **1997**, *36*, 2358.
(30) Erker, G.; Berg, K.; Krüger, C.; Müller, G.; Angermund, K.; Benn, R.; Schroth, G. *Angew. Chem., Int. Ed. Engl.* **1984**, *23*, 455.
(31) Erker, G.; Berg, K.; Angermund, K.; Krüger, C. *Organometallics* **1987**, *6*, 2620.
(32) Lavoie, G. G.; Bergman, R. *G. Angew. Chem.* **1997**, *109*, 2555.
(33) Lavoie, G. G.; Bergman, R. G. *Angew. Chem., Int. Ed. Engl.* **1997**, *36*, 2450.
(34) Skoog, S. J.; Mateo, C.; Lavoie, G. G.; Hollander, F. J.; Bergman, R. G. *Organometallics* **2000**, *19*, 1406.
(35) Wilke, G. *Angew. Chem.* **1963**, *75*, 10.
(36) Wilke, G.; Bogdanovic, B.; Hardt, P.; Heimbach, P.; Keim, W.; Kröner, M.; Oberkirch, W.; Tanaka, K.; Steinrücke, E.; Walter, D.; Zimmerman, H. *Angew. Chem.* **1966**, *78*, 157.
(37) Wilke, G. In *Fundamental Research in Homogeneous Catalysis*; Tsutsui, M., Ed.; Plenum: New York, 1979; Vol. 3, p 1−24.
(38) Davies, S. G. *Organotransition Metal Chemistry: Application to Organic Synthesis*; Pergamon: Oxford, U.K., 1982.
(39) Trost, B. M. *J. Organomet. Chem.* **1986**, *300*, 263.
(40) Tsuji, J. *J. Organomet. Chem.* **1986**, *300*, 281.
(41) Perry, D. C.; Farson, F. S.; Schoenberg, E. *J. Polym. Sci.* **1975**, *13*, 1071.
(42) Quirk, R. P. *Transition Metal Catalyzed Polymerizations, Alkenes and Dienes*, Harwood Academic: London, 1983.
(43) Akita, M.; Yasuda, H.; Nagasuna, K.; Nakamura, A. *Bull. Chem. Soc. Jpn.* **1983**, *56*, 554
(44) Bergbreiter, D. E.; Parsons, G. L. *J. Organomet. Chem.* **1981**, *208*, 47.
(45) Reetz, M. T. *Organotitanium Reagents in Organic Synthesis*; Springer-Verlag: Berlin, 1986.
(46) Klei, E.; Tueben, J. H.; de Liefde Meijer, H. J.; Kwak, E. J.; Bruins, A. P. *J. Organomet. Chem.* **1982**, *224*, 327.
(47) Chen, Y.; Kai, Y.; Kasai, N.; Yasuda, H.; Yamamoto, H.; Nakamura, A. *J. Organomet. Chem.* **1991**, *407*, 191.
(48) Cotton, F. A.; Murillo, C. A.; Petrukhina, M. A. *J. Organomet. Chem.* **2000**, *593−594*, 1.
(49) Martin, H. A.; Jellinek, F. *J. Organomet. Chem.* **1967**, *8*, 115.
(50) Martin, H. A.; Lemaire, P. J.; Jellinek, F. *J. Organomet. Chem.* **1968**, *14*, 149.

ized Zr(III) complexes in the literature are very few.[51] So far, 19 binuclear, 3 neutral mononuclear, and 2 metalate Zr(III) complexes have been structurally characterized. The relative abundance of binuclear complexes indicates their inherent tendency to dimerize so that these species can acquire a coordinative saturation. When sterically hindered ligands were used, mononuclear Zr(III) complexes were obtained and characterized by solid-state X-ray crystallography: e.g., [Zr(η-$C_5H_3{}^tBu_2$-1,3)$_2$Cl],[52] [Zr(η-Cp*)(η-C_8H_8)],[53] [Zr(η-Cp*)-{$NSiMe_2CH_2P^iPr_2$}(CH_2TMS)].[54]

For Zr(III) complexes containing an allyl moiety, Soleil and Choukroun reported that in the Negishi system [Cp_2ZrCl_2·2LiBu] allylic intermediates are present, as identified by ESR and NMR analysis.[55] Interestingly, no solid-state characterizations of Zr(III)−allyl complexes have been reported in the literature.

In a few communications from this laboratory we have shown recently that racemic mixtures of cationic heteroallylic octahedral early-transition-metal complexes are active catalysts for the stereoregular polymerization of olefins.[13−15,27] In addition, we have shown for propylene that, when a cationic Zr complex catalyzes the reaction, a highly stereoregular polypropylene was obtained, whereas with the corresponding Ti cationic complex, an elastomeric polypropylene was produced.[27b] On the basis of those previous results it was remarkably attractive and conceptual important to find a route to synthesize *simple monomeric early-transition-metal group 4 allyl complexes* and to compare their reactivity to that of the well-characterized heteroallylic complexes. In this paper, we report the synthesis, characterization, and solid-state X-ray structural determination of two bulky bis-allylic Zr(III) and Ti(III) complexes. We present the simple oxidation of both M(III) complexes to their corresponding M(IV) complexes. In addition, we describe the solid-state characterization of the racemic mixture of the dimer of the ligand, a compound that is obtained as a byproduct in the synthesis of the organometallic M(III) complexes and also as the decomposition product when the complexes are reacted with dry oxygen. Furthermore, we present the reactivity of the M(III) complexes in the polymerization of α-olefins (polypropylene, polyethylene) in comparison with that of the corresponding M(IV) complexes. To our knowledge, this is the first report of the structural characterization of a Zr(III) allyl complex.

Experimental Section

Materials and Methods. All manipulations of air-sensitive materials were performed with the rigorous exclusion of oxygen and moisture in flamed Schlenk-type glassware on a dual-manifold Schlenk line or interfaced to a high-vacuum (10^{-5} Torr) line or in a nitrogen-filled Vacuum Atmospheres glovebox with a medium-capacity recirculator (1−2 ppm of O_2). Argon and nitrogen gases were purified by passage through a MnO oxygen-removal column and a Davison 4 Å molecular sieve column. Ether solvents (THF-d_8) were distilled under argon from potassium benzophenone ketyl. Hydrocarbon solvents (toluene-d_8, benzene-d_6) were distilled under nitrogen from Na/K alloy. All solvents for vacuum-line manipulations were stored in vacuo over Na/K alloy in resealable bulbs or freshly distilled prior to use. The Li complex of the ligand ^{t}BuMe$_2$SiCH=CHCH$_2$SiMe$_2{}^t$Bu was prepared according to the published procedure.[56] ^{t}BuMe$_2$SiCl, allyl bromide, tris(4-bromophenyl)aminium hexachloroantimonate, and BuLi (all purchased from Aldrich) and HF (Riedel-de Haen) were used as received without any further purification. ^{t}BuMe$_2$SiF was prepared as reported for other fluorides,[57] and the full characterization is given below. CH_2Cl_2 was freshly distilled over P_2O_5. Propylene was purified by passage through a MnO oxygen-removal column and a Davison 4 Å molecular sieve column. Tetramethylethylenediamine (TMEDA) was dried and distilled over Na/K.

NMR spectra were recorded on Bruker AM 200 and Bruker AM 400 spectrometers. Chemical shifts for ^{1}H NMR and ^{13}C NMR are referenced to the internal solvent resonance and reported relative to tetramethylsilane. ^{19}F NMR spectra were referenced to $CFCl_3$. The polypropylene NMR experiments were conducted in a 4:1 (v/v) mixture of 1,2,4-trichlorobenzene and DMSO-d_6 at 135 °C; pentad analysis was performed according to the published literature.[58] ESR experiments were performed at the Ben Gurion University of the Negev at Beersheva, Israel. Melting points of the polymers were measured by DSC (Polymer Laboratories) from the second heating thermogram (heating rate 5 °C/min). The microanalytical laboratory at the Hebrew University of Jerusalem performed elemental analysis. Molecular weight determinations of the polymers were measured on a GPC instrument (TOSOH HLC-8121GPC/HT) using *o*-dichlorobenzene as a solvent at 140 °C. Polystyrene standards were used for the standard calibration curve of the GPC.

Synthesis of ^{t}BuMe$_2$SiF. Since no characterization data are given in the literature for ^{t}BuMe$_2$SiF, which is an intermediate in the synthesis of the lithium complex of the ligand, we present here the full synthetic procedure and the corresponding characterization.

The compound ^{t}BuMe$_2$SiF was prepared by reacting 40 g (0.265 mol) of ^{t}BuMe$_2$SiCl with 133 g (3.192 mol) of 48% (wt) HF in a polypropylene container in a well-ventilated hood with vigorous stirring at room temperature over 16 h. The oily fraction was separated using a polypropylene separation funnel, washed several times with distilled water until no HF was detected, and dried with anhydrous Na_2SO_4. The oily layer was filtered and the ^{t}BuMe$_2$SiF distilled. Yield: 95%. Bp: 112 °C. ^{1}H NMR (298 K, C_6D_6): δ 0.016 (s, 3H, SiCH_3), 0.034 (s, 3H, SiCH_3), 0.869 (s, 9H, C(CH_3)$_3$). ^{13}C NMR (298 K, C_6D_6): δ −4.7 (SiCH$_3$), −4.6 (SiCH$_3$), 18.1 (CMe$_3$), 25.3 (C(CH$_3$)$_3$). ^{19}F NMR (298 K, C_6D_6): δ −170.35. MS: m/z 134 (M^+), 77 (M^+ − C_4H_9), 73 $(CH_3)_2CHSiH_2^+$).

Synthesis of [{(^{t}BuMe$_2$SiCH)$_2$CH}$_2$Zr(μ-Cl)$_2$Li·TMEDA] (1). To a stirred solution of 0.598 g (2.55 mmol) of $ZrCl_4$ in 50 mL of toluene was added 2.003 g (5.1 mmol) of the (^{t}BuMe$_2$-SiCH)$_2$CHLi·TMEDA complex in small portions from a solid addition tube at −78 °C. The reaction mixture was stirred for 1 h at −78 °C and warmed to room temperature; at this temperature the reaction mixture was stirred for 16 h. The reaction mixture was filtered through a frit (No. 3) to remove LiCl, and the resulting clear brown solution was evaporated to dryness by vacuum. The obtained solids were washed with hexane (30 mL × 5) to remove excess TMEDA. The compound was recrystallized twice with toluene at −25 °C to obtain 1.01

(51) Ryan, E. J. In *Comprehensive Organometallic Chemistry II*; Abel, E. W., Stone, F. G. A., Wilkinson, G., Eds.; Lappert, M. F., Vol. Ed.; Pergamon: Oxford, U.K., 1995; Vol. 4, Chapter 8, p 465.
(52) Urazowski, I. F.; Ponomaryev, V. I.; Nifant'ev, I. F.; Lemenovskii, D. A. *J. Organomet. Chem.* **1989**, *368*, 287.
(53) Rogers, R D.; Teuben, J. H. *J. Organomet. Chem.* **1989**, *359*, 41.
(54) Fryzuk, M. D.; Mylvaganam, M. *J. Am. Chem. Soc.* **1993**, *115*, 10360.
(55) Soleil, F.; Choukroun, R. *J. Am. Chem. Soc.* **1997**, *119*, 2938.
(56) Hitchcock, P. B.; Lappert, M. F.; Leung, W. P.; Liu, D. S.; Mak, T. C. W.; Wang, Z. X. *J. Chem. Soc., Dalton Trans.* **1999**, 1257.
(57) Marans, N. S.; Sommer, L. H.; Whitmore, F. C. *J. Am. Chem. Soc.* **1951**, *73*, 5127.
(58) Ewen, J. A. *J. Am. Chem. Soc.* **1984**, *106*, 6355.

g (48% yield) of a brown microcrystalline complex. Single crystals for X-ray diffraction were obtained by recrystallizing the solid from either toluene or hexane at −25 °C. Anal. Found: C, 54.63; H, 10.05; N, 3.61; Cl, 7.61. Calcd (from $C_{36}H_{82}Cl_2LiN_2Si_4Zr \cdot 0.5C_7H_8$ (869.60)): C, 54.55; H, 9.88; N, 3.22; Cl, 8.16.

Synthesis of [{(^{t}BuMe$_2$SiCH)$_2$CH}$_2$Ti(μ-Cl)$_2$Li·TMEDA] (2). To a stirred solution of 1.055 g (5.56 mmol) of $TiCl_4$ in 50 mL of toluene was added 4.368 g (11.1 mmol) of (^{t}BuMe$_2$SiCH)$_2$CHLi·TMEDA in small portions from a solid addition tube for 0.5 h at −78 °C. The reaction mixture was stirred for 1 h at low temperature, and then the mixture was stirred for an additional 16 h, warming the reaction mixture to room temperature. The precipitated LiCl was filtered by means of a frit (No. 3) and the resulting clear chocolate-colored filtrate evaporated to dryness by vacuum. The solids were washed with hexane (30 mL × 5) to remove excess TMEDA, and the hexane removed by vacuum. The solids were dissolved in toluene and slowly cooled to −25 °C, and the precipitate was filtered and dried under vacuum to obtain 2.0 g (∼42%) of a reddish brown (brick red) microcrystalline complex. Single crystals for X-ray diffraction were obtained by recrystallization of the solids from either toluene at −25 °C or from benzene at 0 °C. Anal. Found: C, 59.31; H, 11.01; N, 2.89. Calcd (from $C_{36}H_{82}Cl_2LiN_2Si_4Ti \cdot C_7H_8$ (873.48)): C, 59.12; H, 10.30; N, 3.20.

Isolation of (^{t}BuMe$_2$SiCH=CHCH(SiMe$_2$^{t}Bu)CH-(SiMe$_2$^{t}Bu)CH=CH(SiMe$_2$^{t}Bu) (3). A 20 mL solution of toluene containing 0.5 g (0.572 mmol) of {(^{t}BuMe$_2$SiCH)$_2$-CH}$_2$Ti(μ-Cl)$_2$Li·TMEDA was heated for 0.5 h at 60 °C in a water bath, and dry oxygen was bubbled through the solution. The oxidation starts almost immediately, as observed by the precipitation of LiCl, which was removed by filtration through a frit (No. 3), and the organic layer was concentrated and cooled to −40 °C. The organic dimer of the ligand was obtained (0.24 g, 80%) as colorless crystals from this mother liquor. The GC-MS of the crystals shows a distribution of 77.2%:22.8% for the racemic:meso ratio, respectively. The crystalline racemic dimer was used as the standard for the characterization of the corresponding meso compound. Anal. Found: C, 66.9; H, 12.54. Calcd (from $C_{30}H_{66}Si_4$ (538.36)): C, 66.87; H, 12.26. ^{1}H NMR (298 K, C_6D_6): δ ∼0.09−0.14 (s, 24H, 4SiMe$_2$), 0.98−1.06 (s, 36H, 4Si^{t}Bu), 2.43 (d, 2H, J = 10.3 Hz, C*H*C=C), 5.69 (d, 2H, J = 18.4 Hz, SiC*H*=C), 6.33 (dd, 2H, J_{HH} = 10.3 Hz, J_{HH} = 18.4 Hz, C*H*=C−Si). ^{13}C NMR (298 K, C_6D_6): δ −6.0 (Si*C*H$_3$), −5.8 (Si*C*H$_3$), 16.6 (*C*CH$_3$), 18.1 (CH$_3$), 26.5 (C*C*H$_3$), 27.4 (C*C*H$_3$), 36.4 (*C*HC=C), 126.6 (H*C*=CC), 149.2 (C=*C*HC). GC-MS: m/z 538 (M^+), 393, 365, 351, 263, 221.

Synthesis of {(^{t}BuMe$_2$SiCH)$_2$CH}$_2$ZrCl$_2$ (4). To a stirred solution of 0.500 g (0.57 mmol) of [{(^{t}BuMe$_2$SiCH)$_2$CH}$_2$Zr(μ-Cl)$_2$Li·TMEDA] (**1**) in 30 mL of CH_2Cl_2 was added 0.46 g (0.57 mmol) of (4-Br-C_6H_4)$_3$N$SbCl_6$ dissolved in 20 mL of CH_2Cl_2 dropwise at −78 °C. The reaction mixture was stirred for 1 h at −78 °C and warmed to room temperature; at this temperature the reaction mixture was stirred for 4 h. The reaction mixture was filtered through a frit (No. 3) filled with dry and degassed Celite to remove LiCl, and the resulting brown solution was evaporated to dryness by vacuum to eliminate $SbCl_5$ and TMEDA. The obtained solids were dissolved in toluene (2 mL), and to this solution was added 30 mL of hexane to precipitate a light yellow powder of the zirconium complex. The recrystallization was carried out at −50 °C three times to obtain 91 mg (23%) of clean compound. Anal. Found: C, 51.18; H, 9.63; Cl, 10.54. Calcd (from $C_{30}H_{66}Cl_2Si_4Zr$ (701.32)): C, 51.38; H, 9.49; Cl, 10.11. ^{1}H NMR (298 K, d_8-THF): δ 0.00 (s, 6H, SiMe$_2$), 0.029 (s, 6H, SiMe$_2$), 0.04 (s, 6H, SiMe$_2$), 0.07 (s, 6H, SiMe$_2$), 0.88 (s, 9H, Si^{t}Bu), 0.91 (s, 9H, Si^{t}Bu), 0.92 (s, 9H, Si^{t}Bu), 0.95 (s, 9H, Si^{t}Bu), 2.15 (s, 12H, NCH$_3$), 2.31 (s, 4H, NCH$_2$), 5.55 (d, 2H, J = 18.4 Hz, C*H*CH=CH), 5.60 (d, 2H, J = 18.4 Hz, C*H*=CHCH), 6.25 (m, 2HCHC*H*=CH). ^{13}C NMR (298 K, C_6D_6): δ −6.7 (Si*C*H$_3$), −6.0 (Si*C*H$_3$), −4.3 (Si*C*H$_3$), −3.6 (Si*C*H$_3$), 26.4 (C*C*H$_3$), 26.5 (C*C*H$_3$), 27.4 (C*C*H$_3$), 27.5 (C*C*H$_3$), 16.6 (*C*CH$_3$), 18.2 (*C*CH$_3$), 21.0 (*C*CH$_3$), 25.0 (*C*CH$_3$), 46.4 (*N*CH$_3$), 57.1 (N*C*H$_2$), 124.3 (*C*H), 125.3 (CH), 151.8 (*C*H).

Synthesis of {(^{t}BuMe$_2$SiCH)$_2$CH}$_2$TiCl$_2$ (5). To a stirred solution of 0.250 g (0.28 mmol) of [{(^{t}BuMe$_2$SiCH)$_2$CH)}$_2$Ti(μ-Cl)$_2$Li·TMEDA] (**1**) in 20 mL of CH_2Cl_2 was added 0.23 g (0.28 mmol) of (4-Br-C_6H_4)$_3$N$SbCl_6$ dissolved in 20 mL of CH_2Cl_2 dropwise at −78 °C. The reaction mixture was stirred for 2 h at −78 °C and warmed to room temperature; at this temperature the reaction mixture was stirred for 16 h. The reaction mixture was filtered through a frit (No. 3) filled with dry and degassed Celite to remove LiCl, and the resulting dark red solution was evaporated to dryness by vacuum to eliminate $SbCl_5$ and TMEDA. The obtained solids were dissolved in toluene (2 mL); the solution was cooled to −50 °C and to this solution was added 30 mL of hexane to precipitate an orange powder. Recrystallization of the powder was carried out three times to obtain 20 mg (11%) of clean compound. Anal. Found: C, 55.18; H, 9.98; Cl, 11.04. Calcd (from $C_{30}H_{66}Cl_2Si_4Ti$ (657.96)): C, 54.76; H, 10.11; Cl, 10.78. ^{1}H NMR (298 K, d_8-THF): δ 0.026 (s, 6H, SiMe$_2$), 0.044 (s, 6H, SiMe$_2$), 0.058 (s, 6H, SiMe$_2$), 0.067 (s, 6H, SiMe$_2$), 0.88 (s, 4H, Si^{t}Bu), 0.91 (s, 8H, 2Si^{t}Bu), 0.92 (s, 4H, Si^{t}Bu), 1.01 (s, 4H, Si^{t}Bu), 2.15 (s, 12H, NCH$_3$), 2.30 (s, 4H, NCH$_2$), 5.49 (d, 2H, J = 18.4 Hz, C*H*CHCH), 5.60 (d, 2H, J = 18.4 Hz, C*H*CHCH), 6.22 (m, 2HCHC*H*CH). ^{13}C NMR (298 K, C_6D_6): δ −5.7 (Si*C*H$_3$), −5.6 (Si*C*H$_3$), −3.9 (Si*C*H$_3$), −3.2 (Si*C*H$_3$), 17.0 (*C*CH$_3$), 18.7 (*C*CH$_3$), 26.8 (C*C*H$_3$), 26.9 (C*C*H$_3$), 27.8 (C*C*H$_3$), 27.9 (C*C*H$_3$), 46.4 (N*C*H$_3$), 57.1 (N*C*H$_2$), 124.7 (*C*H), 127.6 (*C*H), 149.6 (*C*H), 152.2 (*C*H).

Ethylene Polymerization Procedure. A 100 mL flame-dried round-bottomed reaction flask equipped with a strong magnetic stirrer was charged with 5 mg of catalyst and the required amount of MAO in the glovebox. The reaction vessel was connected to a high-vacuum line, pumped down, and back-filled with argon three times, the flask was then reevacuated, and a measured amount of toluene (10 mL) was vacuum-transferred. Gaseous ethylene was then admitted to the reactor vessel, after temperature equilibration, through a gas purification column. The gas pressure was maintained at 1 atm throughout the reaction period by means of a pressure manometer. The polymerization was stopped by injecting 25 mL of a methanol−HCl solution into the open reactor in a well-ventilated hood. The formed polyethylene was filtered off, washed with acetone and hexane, and dried under vacuum.

For the polymerizations carried out under high pressure, a 100 mL high-pressure stainless steel reactor with a strong magnetic stirrer was connected to a high-vacuum line. The ethylene was condensed into the reactor at low temperature by freezing the reactor with liquid nitrogen (78 K), and the vessel was then warmed to room temperature. The polymerization was quenched immediately by exhausting the excess ethylene in the well-ventilated hood, followed by quenching of the reaction with the fast addition of 30 mL of 1:1 (v/v) methanol and HCl solution. The collection of the polymer was performed as detailed for the polymerization carried out at atmospheric pressure.

Propylene Polymerization. A 100 mL heavy-walled glass reactor equipped with a strong magnetic stirrer was flame-dried under vacuum and charged with 5 mg of a catalyst and the required amount of MAO in the glovebox. The reactor was connected to a high-vacuum line, and 7 mL of the required solvent was vacuum-transferred. Purified propylene gas was condensed in excess (30 mL) into the reactor vessel by cooling the reactor to 78 K with liquid nitrogen. The reactor was inserted into a thermostated bath to attain equilibration to the desired polymerization temperature, and the polymerization was conducted with strong stirring for the required reaction time. The polymerization was quenched immediately by exhausting the excess propylene in a well-ventilated hood,

Table 1. Crystal Data and Structure Refinement Details for Complexes 1 and 2 and the Dimer of the Ligand 3

	1	2	3
empirical formula	$C_{36}H_{82}Cl_2LiN_2Si_4Zr$	$C_{36}H_{82}Cl_2LiN_2Si_4Ti\cdot0.5C_6H_6$	$C_{30}H_{66}Si_4$
fw	824.46	820.19	539.19
temp, K	230(2)	230(2)	230(2)
wavelength, Å	0.7107	0.710 73	0.710 73
crystal system, space group	monoclinic, $P2_1/n$	triclinic, $P\bar{1}$	monoclinic, $C2/c$
unit cell dimens			
a, Å	17.9150(7)	13.1156(10)	19.0594(10)
b, Å	13.9800(6)	19.413(2)	10.8590(5)
c, Å	20.3530(12)	23.503(3)	18.7038(10)
α, deg	90	71.457(5)	90
β, deg	98.168(2)	79.978(7)	104.922(3)
γ, deg	90	72.761(7)	90
V, Å^3	5045.7(4)	5397.5(10)	3740.5(3)
Z; calcd density, Mg m^{-3}	4; 1.085	4; 1.009	4; 0.957
abs coeff, mm^{-1}	0.442	0.370	0.174
F(000)	1780	1792	1208
cryst size, mm	0.1 × 0.14 × 0.18	0.08 × 0.12 × 0.15	0.12 × 0.16 × 0.20
θ range for data collecn, deg	1.42−27.50	1.25−24.00	2.18−25.50
limiting indices	$0 \le h \le 22$, $0 \le k \le 17$, $-26 \le l \le 26$	$0 \le h \le 15$, $-20 \le k \le 22$, $-25 \le l \le 25$	$0 \le h \le 23$, $0 \le k \le 13$, $-22 \le l \le 21$
no. of rflns collected/unique (R(int))	10 315/10 315 (0.0000)	11 303/11 303 (0.0000)	3481/3481 (0.0000)
completeness to highest θ, %	89.0	66.8	99.9
refinement method		full-matrix least squares on F^2	
no. of data/restraints/params	10 315/0/497	11 303/0/833	3481/0/286
goodness of fit on F^2	0.828	0.727	1.017
final R indices ($I > 2\sigma(I)$)	R1 = 0.0465, wR2 = 0.1169	R1 = 0.0746, wR2 = 0.1677	R1 = 0.0445, wR2 = 0.1188
R indices (all data)	R1 = 0.1374, wR2 = 0.1337	R1 = 0.3104, wR2 = 0.2032	R1 = 0.0711, wR2 = 0.1246
largest diff peak and hole, e Å^{-3}	0.304 and −0.487	0.528 and −0.415	0.318 and −0.181

Scheme 1. Synthetic Route for the Synthesis of Complexes 1 and 2

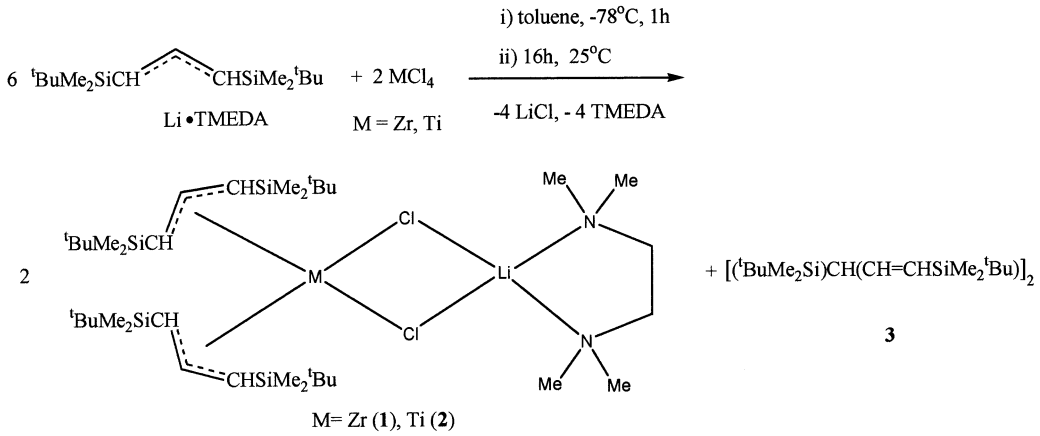

followed by quenching of the reaction with the fast addition of 30 mL of 1:1 (v/v) methanol and HCl solution. The resulted polypropylene was filtered and washed several times with hexane and acetone. The polymer was then dissolved in hot Decalin (130 °C), the solution was filtered, and precipitation was induced from cold acetone. The polymer was dried under high vacuum for several hours.

X-ray Crystallography Procedure. X-ray crystallographic experiments were carried out on a Nonius Kappa CCD diffractometer with graphite-monochromatized Mo Kα radiation (λ = 0.710 73 Å). Crystals were placed in Paratone N oil in a glovebox. Single crystals were mounted on the diffractometer under a stream of cold N_2 at 230 K. Data collection and reduction and cell refinements were carried out with the Nonius software package.[59] The structure's solution and refinement were carried out with the SHELXS-97[60] and SHELXL-97[61] software packages, respectively. The ORTEP program incorporated in the TEXRAY Structure Analysis Package was used for molecular graphics.[62] Relevant crystallographic information is summarized in Table 1.

Results and Discussion

Synthesis and Characterization of Complexes 1 and 2. The reaction of early-transition-metal halides MCl_4 (M = Zr, Ti) with 2 equiv of the lithium allyl compound (^{t}BuMe$_2$SiCH)$_2$CHLi·TMEDA in toluene (Scheme 1) yielded the corresponding reduced complexes [{(^{t}BuMe$_2$SiCH)$_2$CH}$_2$M(μ-Cl)$_2$Li·TMEDA] (M = Zr (**1**), Ti (**2**)), which were isolated as air-sensitive dark brown

(59) Nonius (1997) Kappa CCD Collect Program for data collection and HKL, Schalepack, and Denzo (Otwinowski and Minor, 1997) software package for data reduction and cell refinement.

(60) Sheldrick, G. M. *Acta Crystallogr.* **1990**, *A46*, 467.

(61) Sheldrick, G. M. SHELXL97: Program for the Refinement of Crystal Structures; University of Göttingen, Göttingen, Germany, 1997.

(62) ORTEP: TEXRAY Structure Analysis Package; Molecular Structure Corp., 3200 Research Forest Drive, The Woodlands, TX 77381, 1999.

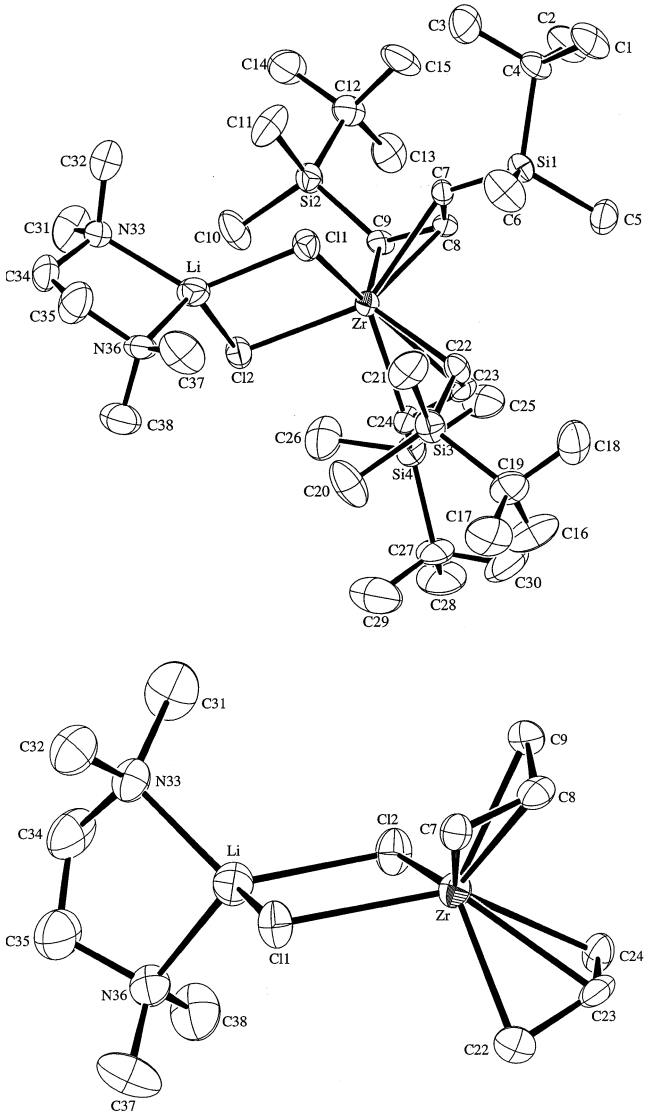

Figure 1. ORTEP diagrams (30% probability ellipsoids) of complex **1** (a, top) showing all non-hydrogen atoms and (b, bottom) showing the ligation around the metal for clarity.

(Zr) and brick red (Ti) crystals in 48% and 42% yields, respectively, with the concomitant formation of the dimer of the allyl ligand (**3**) in 50% yield. An ESR study of the Zr complex (**1**) confirmed its paramagnetic character. At room temperature, an unusually strong singlet, a symmetric Lorentzian line with g(iso) = 1.989 ± 0.003 and ΔH_{pp} = 0.498 ± 0.005 mT, was observed. A similar result was also observed by Soleil and Choukroun for the Zr(III) allyl species in the Negishi system [Cp_2ZrCl_2·2LiBu].[55] The effective magnetic moment of the zirconium complex (μ_{eff} = 1.5 ± 0.8 μ_B) was measured in toluene using the Evans method,[63] indicating almost a complete unpaired electron with almost no metal−metal interactions in solution.

The chemical connectivity of complex **1** was confirmed by an X-ray crystal structure (Figure 1, Tables 1 and 2). The compound crystallized in the monoclinic space group $P2_1/n$.

Table 2. Selected Interatomic Bond Distances (Å) and Angles (deg) of the Zr Complex 1

Bond Distances			
Zr−C(7)	2.474(4)	C(7)−C(8)	1.393(6)
Zr−C(8)	2.415(4)	C(8)−C(9)	1.444(6)
Zr−C(9)	2.361(4)	C(22)−C(23)	1.442(6)
Zr−C(22)	2.369(4)	C(23)−C(24)	1.385(6)
Zr−C(23)	2.396(4)	Li−Cl	2.338(9)
Zr−C(24)	2.436(4)	Li−Cl(2)	2.306(9)
Zr−Cl(2)	2.56(12)	Li−N(33)	2.075(9)
Zr−Cl(1)	2.55(13)	Li−N(36)	2.062(9)

Bond Angles			
C(7)−C(8)−C(9)	122.6(4)	C(22)−Zr−C(24)	62.06(15)
C(22)−C(23)−C(24)	122.4(4)	Cl(1)−Li−Cl(2)	93.0(3)
Cl(1)−Zr−Cl(2)	82.45(4)	N(33)−Li−N(36)	88.2(4)
C(8)−Zr−Cl(1)	115.91(12)	Li−Cl(2)−Zr	91.8(2)
C(23)−Zr−Cl(1)	132.29(12)	Li−Cl(1)−Zr	92.8(2)
C(7)−Zr−C(9)	61.91(14)		

Complex **1** is heterodinuclear, with a Zr(III) and a lithium atom bridged by two Cl atoms. Zr(III) resides in an pseudo-octahedral environment formed by four terminal allylic carbons and two bridging chlorine atoms. The most important feature of this allylic complex is the unsymmetrical disposition of the allylic carbons to the metal center. One of the terminal carbons in each allyl group is closer and equidistant to the metal center than the other two carbons (Zr−C(9) = 2.361Å, Zr−C(8) = 2.415 Å, Zr−C(7) = 2.474 Å and Zr−C(22) = 2.369 Å, Zr−C(23) = 2.396Å, Zr−C(24) = 2.436 Å), creating an unbalanced C=C bond length within each allylic moiety (C(9)−C(8) = 1.444 Å, C(8)−C(7) = 1.393 Å and C(22)−C(23) = 1.442Å, C(23)−C(24) = 1.385 Å).

Interestingly, the same observation for an unsymmetrical σ,π-type (η^3-allyl) bonding has been reported for the allylic ligation in $CpZr(allyl)_3$, showing a difference of 0.182 Å between the distances of the two terminal allylic carbons from the metal center. In the $CpZr(allyl)_3$ complex the longer bond length between the metal and a terminal allylic carbon is 2.624 Å, as compared to 2.474 Å for the corresponding bond in complex **1**. This difference of 0.15 Å between those similar bonds in both complexes is in agreement with the expected values for a difference in oxidation state.[64] Two nitrogen atoms of the TMEDA molecule and two bridging Cl atoms tetrahedrally surround the Li atom in complex **1**: N(36)−Li−N(33) = 88.2(4)°, N(36)−Li−Cl(1) = 115.5(4)°, N(33)−Li−Cl(1) = 126.2(4)°, N(36)−Li−Cl(2) = 121.4(4)°, N(33)−Li−Cl(2) = 115.6(4)°. The $ZrCl_2Li$ core in complex **1** is almost planar (torsion angle Zr−Cl(1)−Li−Cl(2) = 0.0°), and the TMEDA molecule is tilted toward the plane of the $ZrCl_2Li$ core by 78.4°.

The Zr−Cl bond lengths in complex **1** (Zr−Cl(2) = 2.56(12) Å and Zr−Cl(1) = 2.55(13) Å) are slightly smaller as compared to Zr−Cl bonds in homodinuclear Zr(III) complexes that are bridged by one or two chlorine atoms.[65,66] For example, Zr−Cl bond lengths in (η^5:η^5-$C_{10}H_8$)[(η^5-C_5H_5)Zr(μ-Cl)]$_2$ are within the range 2.568−2.591 Å,[65] whereas for ($Cp_2Zr)_2$(μ-Cl)[μ-P(CH_3)$_2$] Zr−Cl bond lengths of 2.595 and 2.587 Å are measured.[66] Hence, as a consequence of the minute difference in Zr−Cl bond lengths, the bond angle Cl(1)−Zr−Cl(2) (82.48°) is smaller than the angles for the corresponding homodinuclear Zr(III) complex (Cl(1)−Zr−Cl(2) = 99.5, 100.5°).[65]

(63) (a) Evans, D. F. *J. Chem. Soc.* **1959**, 2003. (b) *Microscale Inorganic Chemistry*; Safran, Z., Pike, R. M., Singh, M. M., Eds.; Wiley: New York, 1991; Chapter 5.

(64) Shannon, R. D. *Acta Crystallogr.* **1976**, *A32*, 751.
(65) Gambarotta, S.; Chiang, M. Y. *Organometallics* **1987**, *6*, 897.
(66) Chiang, M. Y.; Gambarotta, S. *Organometallics* **1988**, *7*, 1864.

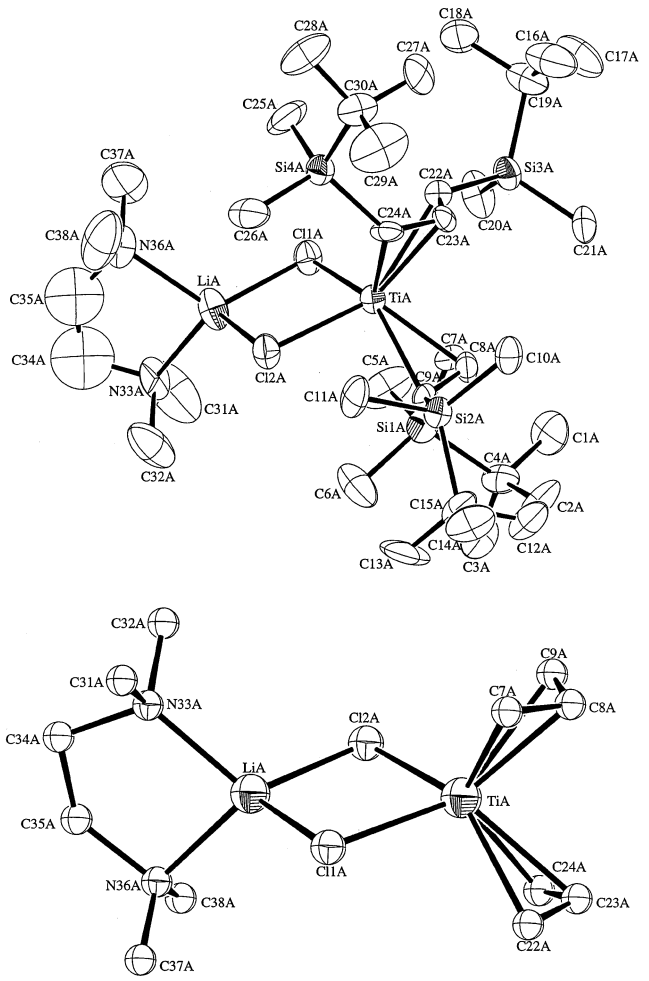

Figure 2. ORTEP diagrams (30% probability ellipsoids) of complex **2** (a, top) showing all non-hydrogen atoms and (b, bottom) showing the ligation around the metal for clarity.

A comparison of the distance formed by the allylic ligand plane and the metal center in complex **1** and in the corresponding lithium salt (^{t}BuMe$_2$SiCH)$_2$CHLi·TMEDA shows that in the former the central carbon of the allylic moiety is remote, as compared to one of the terminal carbons on the same ligand, whereas in the latter the central carbon is closer to the lithium center, as compared to the corresponding allylic terminal carbons.[56] It is worth pointing out that in the lithium salt the orientations of both ^{t}BuMe$_2$Si groups are *exo* with respect to the metal center, whereas for complex **1** in each ligand both ^{t}BuMe$_2$Si groups are arranged in an *exo-endo* fashion.[56]

For complex **2** the effective magnetic moment was measured in THF ($\mu_{eff} = 1.7 \pm 0.7\ \mu_B$), indicating also that almost no metal−metal interactions are present in solution.[63] The molecular structure of complex **2** was confirmed by single-crystal X-ray diffraction analysis (Figure 2, Tables 1 and 3). The deep red crystals crystallized in the triclinic space group $P\bar{1}$, containing two independent units and one molecule of the recrystallization solvent (benzene). Complex **2** is also heterodinuclear, with Ti(III) and lithium atoms bridged by two chlorine atoms. As in complex **1**, both allylic ligands are unsymmetrically arranged around the metal center. In each allylic moiety one terminal allylic carbon is closer to the metal center than the central carbon, which is also closer than the second terminal allylic carbon (Ti−C(7A) = 2.241 Å, Ti−C(8A) = 2.292 Å, Ti−C(9A) = 2.437 Å and Ti−C(24A) = 2.275 Å, Ti−C(23A) = 2.347 Å, Ti−C(22A) = 2.461 Å). This disposition results in different C=C bond lengths (C(7A)−C(8A) = 1.400 Å, C(8A)−C(9A) = 1.385 Å and C(24A)−C(23A) = 1.423 Å, C(23A)−C(22A) = 1.394 Å), indicating again a noticeable distortion toward an unsymmetrical σ,π-type (η^3-allyl) metal complex structure.[31,67−69]

Table 3. Selected Interatomic Bond Distances (Å) and Angles (deg) of the Ti Complex 2

Bond Distances			
Ti(A)−C(7A)	2.241(11)	C(7A)−C(8A)	1.400(2)
Ti(A)−C(8A)	2.292(13)	C(8A)−C(9A)	1.385(12)
Ti(A)−C(9A)	2.437(11)	C(22A)−C(23A)	1.394(16)
Ti(A)−C(22A)	2.461(11)	C(23A)−C(24A)	1.423(12)
Ti(A)−C(23A)	2.347(14)	Li(A)−Cl(1A)	2.280(2)
Ti(A)−C(24A)	2.275(14)	Li(A)−Cl(2A)	2.220(3)
Ti(A)−Cl(2A)	2.438(4)	Li(A)−N(33A)	2.080(3)
Ti(A)−Cl(1A)	2.433(5)	Li(A)−N(36A)	2.190(3)

Bond Angles			
C(7A)−C(8A)−C(9A)	123.9(16)	C(22A)−Ti(A)−C(24A)	62.8
C(22A)−C(23A)−C(24A)	122.6(14)	Cl(1A)−Li(A)−Cl(2A)	95.2(12)
Cl(1A)−Ti(A)−Cl(2A)	86.02(16)	N(33A)−Li(A)−N(36A)	88.2(13)
C(8A)−Ti(A)−Cl(1A)	132.5(4)	Li(A)−Cl(2A)−Ti(A)	90.0(6)
C(23A)−Ti(A)−Cl(1A)	115.0(3)	Li(A)−Cl(1A)−Ti(A)	88.8(8)
C(7A)−Ti(A)−C(9A)	63.3		

The Li atom in complex **2** is also tetrahedrally surrounded by the two nitrogen atoms of the TMEDA molecule and by two chlorine atoms. The $TiCl_2Li$ core is almost planar (torsion angle Ti−Cl(1A)−Li−Cl(2A) = 0.010°), and the TMEDA molecule is close to perpendicular to the $TiCl_2Li$ plane (85.9°). The Ti−Cl bond lengths (Ti−Cl(2A) = 2.438 Å and Ti−Cl(1A) = 2.433 Å) are almost identical with those reported for Ti(III) chloroamido complexes.[70,71] Interestingly, when complex **2** is compared with a similar complex in which the only difference is that the two allylic groups have been replaced by two amido groups, the angle Cl2−Ti−Cl1 is smaller in complex **2** (86.02(16)°) than in the corresponding amido complex (Cl−Ti−Cl = 93.18(5)°).[70] Furthermore, the Ti−Cl−Li angles in complex **2** (Ti−Cl1−Li = 88.80° and Ti−Cl2−Li = 90°) are larger than those observed for the amido complex (83.5 and 84.8°).[70]

The C−C−C bond angles of the allyl ligands in complex **2** (C(22A)−C(23A)−C(24A) = 122.6° and C(7A)−C(8A)−C(9A) = 123.9°) are shorter than those found in either the corresponding lithium salt of the ligand (126.5(6)°)[56] or the recently reported $Ti^{III}(allyl)_2$ complex (125.0, 125.2°)[48] but are within the range (122−127°) reported for complexes of the type $Cp_2Ti(\eta^3$-CHR-CRCHR) (R = H, Me).[47] The orientations of the two ^{t}-BuMe$_2$Si groups are *exo,endo* for each ligand with regard to the metal center, resembling the predilection in complex **1**.

Decomposition of the Allyl Complexes and Characterization of Compound 3. When complexes **1** and

(67) Erker, G.; Dorf, U.; Benn, R.; Reinhardt, R.-D.; Peterson, J. L. *J. Am. Chem. Soc.* **1984**, *106*, 7649.
(68) Highcock, W. J.; Mills, R. M.; Spencer, J. L.; Woodward, P. J. *J. Chem. Soc., Chem. Commun.* **1982**, 128.
(69) Erker, G.; Engel, K.; Dorf, U.; Atwood, J. L.; Hunter, W. E. *Angew. Chem.* **1982**, *94*, 915.
(70) Minhas, R. K.; Scoles, L.; Wong, S.; Gambarotta, S. *Organometallics* **1996**, *15*(4), 1113.
(71) Scoles, L.; Minhas, R. K.; Duchateau, R.; Jubb, J.; Gambarotta, S. *Organometallics* **1994**, *13*(12), 4978.

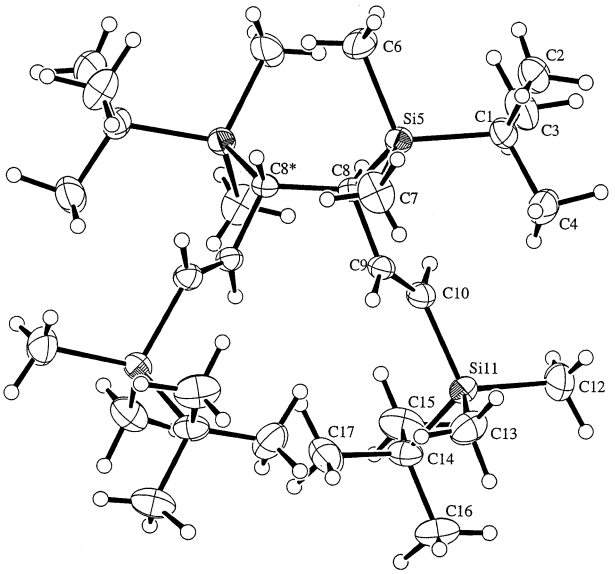

Figure 3. ORTEP diagram (30% probability ellipsoids) of the dimeric compound **3**.

Table 4. Selected Interatomic Bond Distances (Å) and Angles (deg) of Dimer 3

Bond Distances			
C(8*)−C(8)	1.571(4)	Si(5)−C(6)	1.869(3)
C(8)−C(9)	1.504(3)	Si(11)−C(13)	1.865(3)
C(9)−C(10)	1.324(3)	Si(5)−C(1)	1.903(3)
C(8)−Si(5)	1.903(2)	Si(11)−C(14)	1.889(2)
C(10)−Si(11)	1.863(2)		
Bond Angles			
C(8*)−C(8)−C(9)	113.99(11)	C(8)−Si(5)−C(1)	112.65(10)
C(8)−C(9)−C(10)	127.60(2)	C(10)−Si(11)−C(12)	108.02(15)
C(8)−Si(5)−C(7)	107.73(13)	C(10)−Si(11)−C(13)	109.67(13)
C(8)−Si(5)−C(6)	108.63(13)	C(10)−Si(11)−C(14)	109.72(11)

2 are reacted in toluene in the presence of dry oxygen, an oxidation−decomposition reaction starts immediately, shown by a change in color of the reaction mixture, yielding both cases a light yellow solution.[72,73] For complex **2**, cooling the toluene solution to −40 °C allows the formation of colorless white crystals of the organic dimer of the ligand (**3**). The molecular structure of **3** was elucidated by an X-ray crystal structure (Figure 3, Tables 1 and 4). Compound **3** crystallizes in a monoclinic space group with C_2 symmetry. The orientations of the $SiMe_2{}^tBu$ groups in each monomer part are in an *endo-exo* fashion with respect to the corresponding allylic carbon. Interestingly, the decomposition of the complex is highly regioselective, producing mostly the racemic mixture of the dimer (77.2%). The bond length C(8)−C(8)* = 1.571 Å, which is the new bond formed, is slightly longer than the regular C−C single bond (1.54 Å). This may be due to the steric hindrance of the bulky $SiMe_2{}^tBu$ groups. Moreover, in a view through the vector C(8)−C(8*) the substituents on each of the silicon atoms at each side of the vector are in an *anti* configuration, as indicated by the C_2 symmetry of the crystal. It is important to point out that a small fraction (22.8%) of the corresponding meso compound has also been detected by GC-MS and ^1H NMR spectroscopy. The composition and the structure of the racemic and meso forms are also confirmed from both the elemental analysis and ^1H, ^{13}C, $^1H-^{13}C$ correlation, and DEPT NMR studies.

Synthesis of Complexes 4 and 5. Complexes **1** and **2** can be oxidized under mild conditions. The reaction of complexes **1** and **2** with equimolar amounts of $(4\text{-Br-}C_6H_4)_3NSbCl_6$ dissolved in CH_2Cl_2 (eq 1)

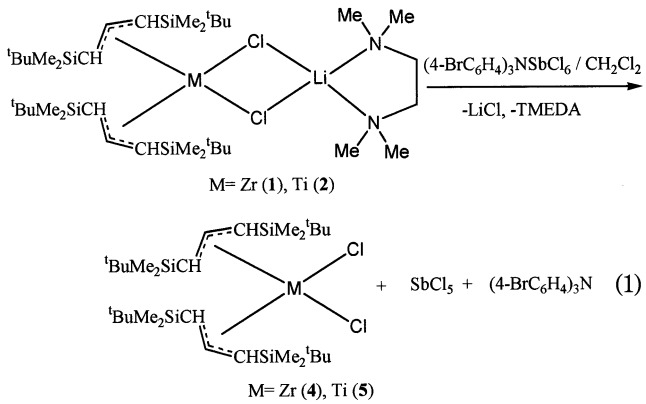

yielded the corresponding dichloro complexes $\{(^tBuMe_2SiCH)_2CH\}_2MCl_2$ (M = Zr (**4**), Ti (**5**)), which were isolated as air-sensitive light yellow (Zr) and orange (Ti) powders, in 23% and 11% yield,s respectively.

The ^1H and ^{13}C NMR spectra of complex **4** exhibit narrow signals. In the ^1H NMR four different signals for each of the $SiMe_2$ groups and each of the ^{t}Bu groups are observed. In addition, three signals for both allylic hydrogens (5.55, 5.60, 6.25 ppm) were detected, indicating that within each allylic moiety similar groups are magnetically different, although the same allylic hydrogens in both ligands are in comparable magnetic environments. A corroboration of the different magnetic environments of the similar groups within each ligand in complex **4** is given in the ^{13}C NMR, exhibiting one signal for each of the $SiMe_2$ groups and each of the ^{t}Bu groups. Likewise, the similarity of the magnetic environments of the allylic carbons in both ligands is confirmed by the appearance of only three signals (124.3, 125.5, and 151.8 ppm).

Although complex **1** and complex **4** are in different oxidation states, it seems, on the basis of the nonsymmetrical NMR results of the latter and the X-ray data of the former, that the ligations on the metal complexes are under similar distortions toward an unsymmetrical σ,π-type (η^3-allyl) metal complex structure.[31,67−69]

For complex **5**, narrow signals are also observed in both ^1H and ^{13}C NMR. The ^1H NMR in THF-d_8 of complex **5** shows the same magnetic environment as observed in complex **4**, creating a signal for each $SiMe_2$ group and each ^{t}Bu group, as well as only three signals for the allylic hydrogens for both ligands. The ^{13}C NMR of complex **5** is more informative than the ^1H NMR. The pattern is the same as that of complex **4**, showing an individual signal for every $SiMe_2$ group and every ^{t}Bu group, although one signal is observed for each of the allylic carbons in a particular ligand, indicating that both ligations are in different magnetic environments. An agreeable confirmation regarding the unsymmetrical arrangement of the ligands is detected by the ^{13}C NMR, exhibiting a signal for every particular carbon in each individual ligand.

(72) Meijere, A.; Stecker, B.; Kourdioukov, A.; Williams, C. M. *Synthesis* **2000**, *7*, 929 and references therein.
(73) Jin, X.; Novak, B. M. *Macromolecules* **2000**, *33*(17), 6205.

Scheme 2. Plausible Routes for the Formation of Complexes 1 and 2

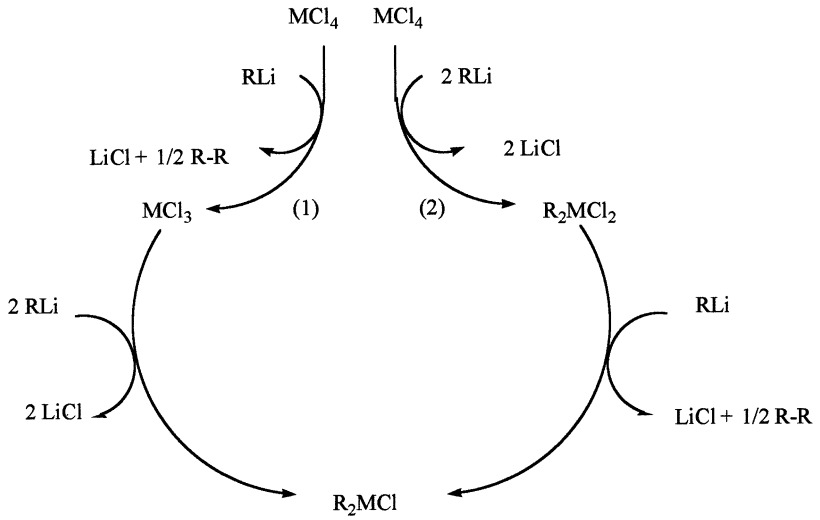

Interestingly, when complex **5** was dissolved in benzene or toluene, rapid interconversion of two compounds was observed in the ^{1}H NMR. These compounds are the η^1- and the η^3-allyl complexes, which are easily distinguished by the appearance of a new set of two doublets (each doublet is for each allylic fraction) at 2.44 and at 2.38 ppm, with J couplings of 10 and 8 Hz, respectively. Cooling the solution to trap one of the species was not possible, although changing the solvent to THF allows the sole formation of the η^3 complex. A similar behavior for complex **4** was not observed at higher or lower temperatures. No considerable changes in the chemical shifts of the allylic protons were perceived in the variable-temperature ^{1}H NMR study of complex **4** over the temperature range from −50 to +50 °C.

It is important to point out that the reaction of complexes **4** and **5** with dry oxygen in toluene at 50 °C produced a myriad of decomposition products, although no dimer **3** was observed.

Formation of the Reduced Complexes. The reduction of both starting metal chloride salts $M^{IV}Cl_4$ (M = Zr, Ti) to their corresponding M(III) oxidation states can be explained by two parallel pathways (Scheme 2). In the first route (1), 1 equiv of the allyllithium complex (RLi) reduces the MCl_4 to MCl_3 with the concomitant formation of the allyl dimer **3** and LiCl. The reaction of MCl_3 with 2 equiv more of the lithium allyl complex yields the corresponding complexes **1** and **2**, for Zr and Ti, respectively. In the second route (2) 2 equiv of the lithium allyl reacts with the MCl_4, yielding the bis(allyl)-metal dichloride. An additional 1 equiv of the lithium allyl complex may reduce the metal, yielding the complexes **1** and **2**, for Zr and Ti, respectively, and dimer **3**. It is important to point out that both mechanisms are in agreement with the yield of the complexes (<50%) and with the concurrent formation of the dimer. In addition, no supporting evidence for mono(allyl) or tris-(allyl) complexes was detected, arguing that disproportionation reactions are not major pathways.[74] To distinguish among both pathways, we have performed the equimolar reaction of either complex **4** or **5** with 1 equiv of the lithium bis(allyl) salt, producing the corresponding tris(allyl) complexes (observed in situ), arguing that under the reaction conditions, if operative, the second route is not the major pathway for the production of complexes **1** and **2**.

Catalytic Polymerization Studies. The catalytic activities of the precatalysts **1** and **2** activated with MAO in the polymerization of propylene are presented in Table 5. For both complexes a minimum MAO: catalyst ratio of 400 was essential to observe any catalytic activity at high monomer concentration (high pressure). Below that ratio or at atmospheric pressure, no polymerization reaction was detected.

One conceptual question arises regarding the oxidation state of the active complex during the polymerization process. If Ti(III) or Zr(III) is the active species instead of a cationic Ti(IV) or Zr(IV), there should be no need for MAO as a cocatalyst. The reaction of complexes **1** and **2** with 1 equiv of MeLi yielded the corresponding methyl complexes (observed in situ), which upon reaction with propylene showed no polymerization activity. Thus, it seems that the complexes may undergo an oxidative coupling with the olefins and then MAO generates the active cationic complexes.[72] To corroborate such a possible oxidation pathway, the catalytic activities of complexes **1** and **4** and of **2** and **5** were compared, under identical reaction conditions, for the polymerization of propylene, to obtain in each case similar amounts of polymer with almost identical stereoregularities and molecular weights (compare entries 4 and 5 or entries 13 and 14 in Table 5). This results argues for cationic M(IV) (M = Zr, Ti) complexes as the active species.

When complex **1** was used as the precatalyst, a medium stereoregular polymer was always observed with a percent *mmmm* content changing on the basis of the polymerization conditions. Increasing the MAO: complex ratio from 400 to 800 (entries 1 and 2 in Table 5) induces an increase in both catalytic activity and molecular weight of the polymer. Further augmentation in the MAO:complex ratio causes a slow decrease in the activity and in the molecular weight of the polymers. These results suggest that the higher the MAO concentration, the faster the operative aluminum transfer

(74) Edelmann, F. T. In *Comprehensive Organometallic Chemistry II*; Abel, E. W., Stone, F. G. A., Wilkinson, G., Eds.; Pergamon Press: Oxford, U.K., 1995; Chapter 2, and references therein.

Table 5. Activity, Molecular Weight and Melting Point Data for the Polymerization of Propylene Using Complexes 1, 2, 4 and 5 activated by MAO[a]

entry	cat.	solvent[b]	MAO[c]	temp (°C)	*P* (atm)	$10^{-4}A$[d]	M_w	M_n	PDI	*mmmm* (%)	mp (°C)
1	**1**	T	400	25	7.2	0.7	41 700	16 000	2.6	61	136
2	**1**	T	800	25	7.2	1.6	83 400	15 700	5.3	56	133
3	**1**	T	800	50	10.1	2.1	29 400	12 400	2.4	96	152
4	**1**	T	1000	25	7.2	1.3	46 300	15 800	2.9	74	138
5	**4**	T	1000	25	7.2	1.2	44 200	15 200	2.9	71	138
6	**2**	T	400	25	7.2	15.0	336 300	113 600	2.9	43	elastomer[e]
7	**2**	T	400	50	10.1	15.3	78 100	140 700	5.5	45	elastomer[e]
8	**2**	T	400	0	5.1	7.2	2 027 600	552 800	3.6	33	elastomer
9	**2**	CH_2Cl_2	400	25	7.2	16.8	66 000	25 000	2.6	44	elastomer[e]
10	**2**	T	500	25	7.2	21.0	193 100	60 800	3.2	44	elastomer[e]
11	**2**	T	600	25	7.2	19.7	141 400	55 600	2.5	27	elastomer
12	**2**	T	800	25	7.2	17.2	159 400	62 700	2.5	17	elastomer
13	**2**	T	1000	25	7.2	15.0	114 600	42 900	2.7	20	elastomer
14	**5**	T	1000	25	7.2	14.7	115 200	42 600	2.7	22	elastomer
15	**2**	T	1200	25	7.2	14.8	85 600	31 100	2.8	15	elastomer

[a] Conditions: catalyst, 5 mg; polymerization time, 1 h. [b] Solvent: T = toluene. [c] MAO/catalyst ratio. [d] *A* = activity in g of PP (mol of catalyst)$^{-1}$ h^{-1}. [e] For all the different marked elastomers a narrow crystallization signal is observed at 90−100 °C, whereas the melting points of the polymers are broad, with an endothermic signal starting at 120 °C.

termination pathway (vide infra). Elevating the temperature from 25 to 50 °C (entries 2 and 3) generates a highly isotactic polymer (96% *mmmm*) with an increase in the catalytic activity and a decrease in the molecular weight of the polymer. The reduction in molecular weight at 50 °C as compared to the molecular weight at 25 °C indicates that the polymer chain is cleaved from the metal center more rapidly at the high temperature. The molecular weight distribution for the polymers catalyzed by precatalyst complex **1** (entries 1−4, Table 5) are low, suggesting that active site uniformity is effective during the polymerization process. The ^{13}C NMR of all the polymers obtained by using complex **1** as the precatalyst presents a higher isotactic signal in combination with other signals, which are representative of an atactic pentad analysis. It is important to point out that the measured polymers were fractionalized previously and no atactic fractions remain in the washing solvents. Moreover, the gel permeation chromatography measurements show exclusively one signal for each polymer. The termination process as expressed by the ^{13}C NMR shows that the aluminum transfer mechanism is the major operative pathway. The NMR displayed only an isobutyl signal for the termination process, while vinylic carbons were not encountered.

Interestingly, when the polymerization with complex **1** was carried out in CH_2Cl_2, catalytic activities were obtained similar to those for the polymerization carried out in toluene, although the polymer was obtained as an elastomer with 34% *mmmm* composition.

Melting points of the polymers (Table 5) are reported as the first peak of the melting endotherms of the second run. The melting temperatures of the polypropylene polymers increase with an increase in the isotactic pentad content (% *mmmm*) of the polymer. The heating curves display very broad melting endotherms with two peaks. The onset of melting points appeared around 125−130 °C and continued up to a peak ranging up to around 160 °C. The cooling curves gave the most reproducible results and revealed only one sharp crystallization exotherm within the range 99−115.6 °C. These results indicate that different domains with different melting points are within the same polymer, as supported by the existence of only one crystallization signal. Because of the broad melting points of the polymers, the mechanical elasticity exhibited by the lower isotactic polymers, and the ^{13}C NMR of the polymers exhibiting a high isotactic signal together with the other nine expected signals for an atactic pentad, in addition to a narrow polydispersity and the appearance of only one signal on the gel permeation chromatography for each polymer, it is plausible to conclude that the polymers are formed by a dynamic complex, giving yield to a copolymer of atactic and isotactic domains. Thus, it seems plausible that only the cationic complex **4** is able to undergo a dynamic $\eta^3 \rightarrow \eta^1$ coordination (complex **4** itself did not show any dynamic behavior). When a η^3 coordination is operative, a cationic racemic octahedral complex is formed, responsible for the polymerization of the isotactic domains, whereas when the coordination is η^1, a cationic tetrahedral complex with a C_{2v} symmetry is obtained, accounting for the atactic domains. To corroborate a dynamic coordination as a function of temperature for the cationic complex **4**, we have performed the reaction of an excess of MAO with complex **4** (MAO:complex = 100), in the range of −50 to 70 °C. The ^1H NMR shows a broad signal in the vinylic region at room temperature that becomes rather sharp at lower temperature, in addition to a broad new signal at 3.2−3.5 ppm corresponding to the expected allylic hydrogens in a dynamic $\eta^3 \rightarrow \eta^1$ cationic system. A similar dynamic process interconverting between tetrahedral (C_{2v}) and octahedral (C_2) coordinations and giving yield to elastomeric polypropylene has been recently observed for titanium and zirconium aminophosphine complexes.[75]

When complex **2** was used as the precatalyst, the activity and the molecular weights of the polymers were higher than those obtained using the precatalyst complex **1**. In contrast to the stereoregular polymers obtained with complex **1**, the polypropylene catalyzed by complex **2**, under all the different reaction conditions, were always found to be elastomers. The ^{13}C NMR of the polymers shows always after fractionalization a high signal corresponding to the isotactic *mmmm* pentad

(75) For a recent publication regarding $\eta^3 \rightarrow \eta^1$ dynamic coordination and its effect on the polymerization of propylene, see ref 27a and: (a) Plat, D. The Reactivity of Group IV Aminophosphine Complexes. Ph.D. Thesis, Technion, Haifa, Israel, 2000. (b) Shaviv, E. Heteroallylic Early Transition Metal Complexes. M.Sc. Thesis, Technion, Haifa, Israel, 2000.

analysis together with the nine signals for an atactic domain. The dominant termination process operative, as manifested by the ^{13}C NMR, is the aluminum transfer mechanism, as was encountered for precatalyst complex **1**. It is important to point out that the gel permeation chromatography of the polymers shows only one signal, indicating that no high-molecular-weight atactic polymers were present.

The effect of the amount of MAO on the polymerization activity catalyzed by precatalyst **2** (entries 6 and 9−14) indicates that a maximum activity was observed at a MAO:metal ratio of about 500. A higher MAO ratio brings the reaction to an activity plateau. This trend is indeed distinct from the results reported in the literature for analogous cyclopentadienyl early-transition-metal systems.[76] The effect of MAO on the molecular weight of the polymers indicates that the higher the MAO:complex ratio, the lower the molecular weight of the polymers when the polydispersity remains almost constant. This result indicates that the cocatalyst concentration is catalyzing possible alkyl transfer pathways, terminating the chain propagation.[77] It is worth noting that the higher the MAO:metal ratio, the lower the isotactic *mmmm* pentad content on the polymers, leveling off at about *mmmm* = 15%, which is far higher than the statistical *mmmm* value for an atactic polymer (6%). The effect of the temperature on the polymerization process causes a radical change in the properties of the polymers (entries 6−8, Table 5). When the polymerization is carried out at 0 °C, an extremely high molecular weight elastomeric polypropylene was obtained (2×10^6 g mol^{-1}). Increasing the temperature to 25 °C causes a slight increase in the catalytic activities, although this induces a low-molecular-weight polymer. Additional elevation in temperature to 50 °C brings about a higher molecular weight polymer with catalytic activity similar to that for the process at 25 °C. These results argue that at low temperature the termination process is rather slow as compared to the insertion process. Increasing the temperature to 25 °C gives rise to a decrease in the molecular weight of the polymers due to a faster termination process (aluminum transfer) that competes with the insertion reaction. A further increase in temperature to 50 °C gives a higher molecular weight polymer, which can be accounted for by the reinsertion of the terminated alkyl chain at the metal center. This process has been recently observed with acetylacetonate group 4 complexes.[26]

Use of CH_2Cl_2 as a solvent with the precatalyst complex **2**, instead of toluene (entries 6 and 9, Table 5), enhances the catalytic activity but decreases by far the molecular weight of the polymer. This phenomenon can be rationalized by the polarity of dichloromethane, which causes a greater charge separation between the cationic metal complex and the anionic methylalumoxane moiety, enabling the monomer insertion process. In addition, dichloromethane itself can act as a chain-transfer reagent, causing the lower molecular weight of the polymers.[26] The similarity of the solvent effect of dichloromethane as compared to that of toluene, in the polymerization of propylene, have been reported.[13,27,78] Due to the low polydispersity of the polymers, the substantial percent *mmmm* composition together with the atactic pentad domains, the appearance of only one type of polymer in the gel permeation chromatography, and the rapid interconversion of the ligand from η^1 to η^3 as observed for complex **5** with benzene at room temperature, it seems plausible that the elastomeric polypropylene is obtained in a fashion similar to that observed for complex **4**. That is, changing the coordination from η^1 to η^3 changes the symmetry of the complex from C_{2v} to C_2, which is responsible for the atactic−isotactic domains in the polymerization reaction.

We have utilized atomic force microscopy (AFM) to discriminate between crystalline and amorphous areas in a homogeneous polymer. The use of AFM in polymer chemistry to differentiate different crystalline regions is well-accepted in the literature, allowing a visual recognition of the different realms.[79] Thus, a sample of elastomeric polypropylene (entry 10, Table 5) was measured at room temperature after casting it over glass (Figure 4). The figure shows brighter lamellar crystalline aggregates that are embedded in amorphous darker areas. The picture corroborates the notion that different crystalline areas cause different melting points (broad signal), even though there is only one narrow crystallization temperature.

For comparison, the catalytic activity of the precatalyst complexes **1**, **2**, **4**, and **5** (complexes **4** and **5** were studied for comparison), activated by methylalumoxane, has been also studied for the polymerization of ethylene to high-density polyethylene (Table 6). For complex **1**, augmenting the ethylene pressure resulted in enlarging the catalytic activity by an order of magnitude (entries 1 and 2, Table 6), although no major effect was observed for the molecular weight or the high polydispersity of the polymer ($\sim 3 \times 10^6$ g mol^{-1}, $M_w/M_n = \sim 15$). This high polydispersity suggests the loss of active site uniformity during the polymerization process. When, under reaction conditions, the activity of complex **1** is compared with that of complex **4**, a higher activity is obtained, although slightly lower molecular weights of the polymers and polydispersities are observed (entries 2 and 3 in Table 6). For complex **2**, raising the concentration of ethylene (entries 4−6) causes an increase in both molecular weight and catalytic activities. Interestingly, the molecular weights of polyethylene catalyzed by this precatalyst are extremely large as compared to the molecular weight of the polymers obtained at atmospheric pressure, reaching 1.35×10^7 g mol^{-1} at 18 atm. Moreover, the polydispersities of the polymers are narrower (3.5−8.5) as compared to the results obtained with the precatalyst complex **1**, indicating also a loss of

(76) (a) Richter, J.; Edelmann, F. T.; Noltemeyer, M.; Schmidt, H.-G.; Shmulinson, M.; Eisen, M. S. *J. Mol. Catal. A: Chem.* **1998**, *130*, 149. (b) Bochmann, M.; Lancaster, S. J. *Organometallics* **1993**, *12*, 633. (c) Okuda, J. *Angew. Chem., Int. Ed. Engl.* **1992**, *31*, 47. (d) Resconi, L.; Abis, L.; Franciscono, G. *Macromolecules* **1992**, *25*, 6814. (e) Yang, X.; Stern, C. L.; Marks, T. J. A. *J. Am. Chem. Soc.* **1994**, *116*, 10015. (f) Collins, S.; Gauthier, W. J.; Holden, D. A.; Kuntz, B. A.; Taylor, N. J.; Ward, D. G. *Organometallics* **1991**, *10*, 2061.

(77) (a) Sinn, H.; Kaminsky, W. *Adv. Organomet. Chem.* **1980**, *18*, 99. (b) Bochmann, M.; Cuenca, T.; Hardy, D. T. *J. Organomet. Chem.* **1994**, *C10*, 484.

(78) Fereres, M. G.; Koch, T.; Hey-Hawkins, E.; Eisen, M. S. *J. Organomet. Chem.* **1999**, *580*, 145.

(79) (a) Ivanov, D. A.; Nysten, B.; Jonas, A. M. *Polymer* **1999**, *40*, 5899. (b) Orefice, R. L.; Brennan, A. *Mater. Res.* **1998**, *1*, 19. (c) Pfau, A.; Janke, A.; Heckmann, W. *Surf. Interface Anal.* **1999**, *27*, 410. (d) Tomasetti, E.; Legras, R.; Nysten, B. *Nanotechnology* **1998**, *9*, 305. (e) Xu, K.; Gusev, A. I.; Hercules, D. M. *Surf. Interface Anal.* **1999**, *27*, 659. (f) Haeringen, D. T. V.; Varga, J.; Ehrenstein, G. W.; Vancso, G. J. *J. Polym. Sci., B: Polym. Phys.* **2000**, *38*, 672.

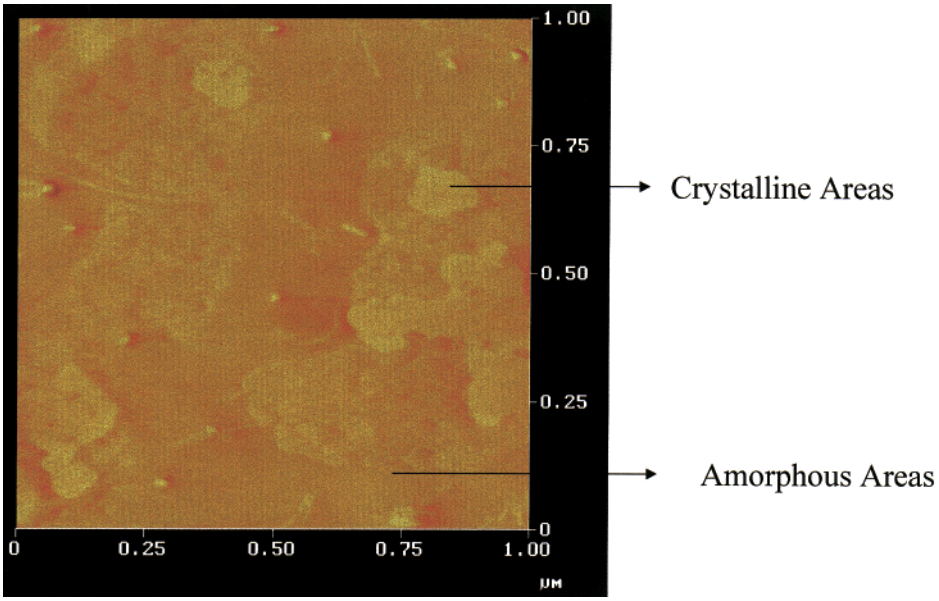

Figure 4.

Table 6. Activity, Molecular Weight, and Melting Point Data for the Polymerization of Ethylene using Complexes 1, 2, 4, and 5 activated by MAO[a]

entry	cat.	*P* (atm)	$10^{-4}A$[b]	M_w	M_n	PDI	mp (°C)
1	1	1	1.5	3 100 000	170 000	18.2	136.8
2	1	30	52.0	2 710 000	181 000	14.9	135.5
2	4	30	122.0	1 850 000	180 000	10.2	135.4
3	2	1	0.5	4 90 000	573 000	8.5	136.9
4	2	18	22.8	13 500 000	2 420 000	5	133.8
5	2	30	22.5	8 180 000	2 280 000	3.5	135.9
5	5	30	78.5	6 420 000	2 350 000	2.7	136.1

[a] Conditions: catalyst, 2 mg; reaction time, 1 h; 7 mL of toluene as solvent at 25 °C; [MAO]:catalyst = 400. [b] Activity in g of PE (mol of catalyst)$^{-1}$ h^{-1}.

active site uniformity. Similar to what is encountered for complex **4**, the comparison of complex **5** with complex **2** (entries 6 and 7 in Table 6) shows larger activities with a small decrease in molecular weights and polydispersities. In general, for both precatalysts **1** and **2**, the higher the pressure (the monomer concentration) the lower the melting points of the polymers, indicating that higher branchings are obtained as a function of the monomer concentration.[80−82] It is important to point out that the oxidation of the precatalysts **1** and **2**, and the concomitant cationic formation of these complexes, under the ethylene polymerization conditions, is much slower as compared to the propylene polymerization conditions, as indicated by the activity of these complexes in both processes.

Conclusions

In conclusion, the first stable bis(allyl)zirconium(III) chloride (**1**) and the isolobal bis(allyl)titanium(III) chloride complex (**2**) have been synthesized and fully characterized, including by solid-state X-ray diffraction. These compounds can be oxidized to their corresponding bis(allyl)zirconium(IV) dichloride (**4**) and bis(allyl)titanium(IV) dichloride complexes (**5**). The catalytic precursor **1** reacts with MAO and propylene, giving rise to the corresponding cationic complex **4**, and stereoregular polymers with atactic and isotactic domains. The precatalyst **2** reacts with MAO and propylene, yielding also the corresponding cationic complex **5** and elastomeric polypropylenes. The elastomeric polymers have been characterized by AFM. Both complexes **1** and **2** are also good precatalysts for the polymerization of ethylene to high-density polyethylene with high molecular weight, and their activities are compared with those of the corresponding complexes **4** and **5**.

Acknowledgment. We thank the reviewers for the stimulating questions raised during the revision of this paper. This research was supported by the Ministry of Science, Goverment of Israel, by The Fund for the Promotion of Research at the Technion, and by the Henry Gutwirth Fund for the Promotion of Research at the Technion. B.R. thanks the Ministry of Science, Government of Israel, for a postdoctoral fellowship. We thank Prof A. I. Shames at the Ben-Gurion University of the Negev for ESR measurements and Dr. Yoav Eichen at the Faculty of Chemistry at the Technion for AFM measurements. We thank Dr. P. Maiti, Prof M. Okamoto, and Prof T. Kotaka at the Toyoto Institute of Technology for GPC measurements.

Supporting Information Available: Tables of final positional parameters and isotropic and anisotropic displacement parameters for all atoms and bond lengths and angles for complexes **1**−**3** and figures giving selected ^{13}C NMR and DSC thermograms for different elastomeric polypropylenes and high-density polyethylene. This material is available free of charge via the Internet at http://pubs.acs.org.

OM0009942

(80) Kim, J. S.; Wojcinski, L. M., II; Liu, S.; Sworen, J. C.; Sen, A. *J. Am. Chem. Soc.* **2000**, *122*, 5668.

(81) The large difference in polydispersity, as observed for complexes **1** and **2** for the different olefins, is not yet clear. Although highly branched polyethylene may give a large polydispersity, this is not the case here. The ^{13}C NMR of the polyethylene measured at 130 °C in 1,2,4-trichlorobenzene shows almost no branching.

(82) Sato, F.; Urabe, H.; Okamoto, S. *Chem. Rev.* **2000**, *100*, 2835 and references therein.